



Robust active suspension control of vehicles with varying vehicle mass

Masahiro Oya¹ · Hiraku Komura¹

Received: 31 July 2023 / Accepted: 30 November 2023 / Published online: 19 January 2024
© International Society of Artificial Life and Robotics (ISAROB) 2024

Abstract

In vehicles with active suspensions, if handling stability is improved strongly by using a LQ controller for a road surface such as large bumps, ride comfort may deteriorate even for a road surface such as not so large bumps. Recently, to avoid the problem, a nonlinear active suspension control scheme has been proposed. However, in the proposed nonlinear controller, it is required that vehicle mass does not vary. In practice, vehicle mass varies greatly. If vehicle mass varies, the controller has to be redesigned. In this paper, to address the problem, based on the proposed nonlinear control scheme, we develop a new robust active suspension control scheme.

Keywords Active suspension system · Handling stability · Ride comfort

1 Introduction

Recently, aiming to improve safety, efficiency, mobility and so on, many researchers have proposed lane following control schemes (for example [1–3]). In the case when the vertical force between wheels and a road surface becomes too small, handling stability becomes worse and good lane following performance cannot be expected. On the other hand, we have to also consider a method to improve ride comfort of autonomous vehicles. To improve both of handling stability and ride comfort of vehicles, based on a quarter vehicle model, various active suspension control schemes [4–14] have been provided. Control schemes [15–17] have been also developed based on a half vehicle model. Based on a full vehicle model, the authors of the reference papers [18–20] have provided controllers.

It is assumed that vehicles run on a highway. If design parameters are set in the controlled vehicles proposed in [4–20] so as to further improve handling stability for a road surface such as large bumps, ride comfort may deteriorate even for a road surface such as that with not so large bumps. Very recently, to address the problem, a nonlinear active suspension control scheme [21] has been proposed. As shown in numerical simulation results of the reference paper [21], even if the relative tire load exceeds a dangerous value in a

passive vehicle, both ride comfort and steering stability can be significantly improved in the controlled vehicle. However, in the nonlinear control scheme, the authors do not consider varying vehicle mass. In the practical case, vehicle mass varies greatly. Using the proposed control scheme [21], we have to redesign a controller every time vehicle mass varies. Until now, many robust active suspension controllers have been proposed (For example [22–24]). As far as authors know, there is no robust control scheme in which both ride comfort and steering stability can be significantly improved.

In the paper, we propose a new robust active suspension control scheme based on a control scheme [21]. In the robust control scheme, even if vehicle mass varies, redesign of a controller is not required. To achieve this, at first, we propose a design method for an ideal vehicle model. In the ideal vehicle model, even if vehicle mass varies, good ride comfort and good handling stability can be achieved by setting only one design parameter. After that, to make the real vehicle track the designed ideal vehicle model, we will develop a robust tracking controller.

2 Dynamic equation

Figure 1 shows a quarter vehicle model. Table 1 shows the explanation of the parameters used in the figure and equations below. The new states are defined by $x_b(t) = z_s(t) - z_r(t)$, $x_t(t) = z_u(t) - z_r(t)$, $\xi(t) = \ddot{z}_s(t)$. Then, we have [21]

✉ Masahiro Oya
oya@cntl.kyutech.ac.jp

¹ Kyushu Institute of Technology, Kitakyushu, Japan

Fig. 1 Quarter vehicle model

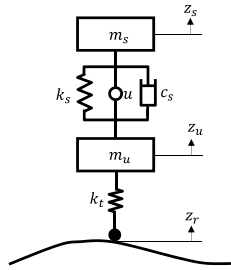


Table 1 Meaning of symbols

m_s, m_u	Sprung mass and unsprung mass
k_s, c_s	Spring stiffness and damping coefficient
k_t	Tire spring stiffness
u	Control force produced by active suspension
z_s, z_u	Displacement of m_s and m_u
z_r	Road displacement

$$\left. \begin{aligned} \dot{\mathbf{x}}(t) &= \mathbf{A}\mathbf{x}(t) + \frac{1}{m_s}\mathbf{b}\mu(t) - \mathbf{d}\ddot{z}_r(t) \\ \mu(t) &= \dot{u}(t) + \alpha u(t), \quad \mathbf{x}(t) = [\mathbf{x}_b(t)^T \quad \mathbf{x}_t(t)^T]^T \\ \mathbf{x}_b(t) &= [\mathbf{x}_b(t) \quad \dot{\mathbf{x}}_b(t) \quad \xi(t)]^T, \quad \mathbf{x}_t(t) = [\mathbf{x}_t(t) \quad \dot{\mathbf{x}}_t(t)]^T \end{aligned} \right\} \quad (1)$$

$$\left. \begin{aligned} \mathbf{A} &= \begin{bmatrix} \mathbf{A}_b & \mathbf{A}_{bt} \\ \mathbf{A}_{tb} & \mathbf{A}_t \end{bmatrix}, \quad \mathbf{A}_b = \Omega_b + \mathbf{b}_b\mathbf{a}_{1b}^T, \quad \mathbf{A}_{bt} = \mathbf{b}_b\mathbf{a}_{1t}^T \\ \Omega_b &= \mathbf{c}_b\mathbf{d}_b^T + \mathbf{d}_b\mathbf{b}_b^T, \quad \mathbf{c}_b = [1 \ 0 \ 0]^T, \quad \mathbf{d}_b = [0 \ 1 \ 0]^T \\ \mathbf{b}_b &= [0 \ 0 \ 1]^T, \quad \mathbf{b} = [\mathbf{b}_b^T \ 0 \ 0]^T, \quad \mathbf{d} = [\mathbf{d}_b^T \ \mathbf{b}_t^T]^T \\ \mathbf{a}_{1b} &= -[\alpha k_{ss} \quad k_{ss} + \alpha c_{ss} \quad c_{ss}(1 + m_{su}) + \alpha]^T \\ \mathbf{a}_{1t} &= [\alpha k_{ss} - c_{ss}k_{tu} \quad k_{ss} + \alpha c_{ss}]^T, \quad \mathbf{b}_t = [0 \ 1]^T \\ c_{ss} &= \frac{c_s}{m_s}, \quad k_{ss} = \frac{k_s}{m_s}, \quad m_{su} = \frac{m_s}{m_u}, \quad k_{tu} = \frac{k_t}{m_u} \\ \mathbf{A}_{tb} &= -m_{su}\mathbf{b}_t\mathbf{b}_b^T, \quad \mathbf{A}_t = \mathbf{c}_t\mathbf{b}_t^T - k_{tu}\mathbf{b}_t\mathbf{c}_t^T, \quad \mathbf{c}_t = [1 \ 0]^T \end{aligned} \right\} \quad (2)$$

where α is a positive design parameter. The signal $\mu(t)$ is the control input to be designed below, and the real control input $u(t)$ is generated by the solution of the second equation of (1).

In this paper, the control objective is to develop a robust active suspension controller against varying sprung mass that satisfies the following conditions [21].

C1 Passenger resonance frequency exists in the neighborhood of 1–2 [Hz]. To improve the ride comfort of passengers, the magnitude of the vertical acceleration of the vehicle body m_s must be reduced to as small as possible with respect to the road surface displacement frequency neighborhood of 1–2 [Hz].

C2 To achieve good handling stability, the vehicle must be controlled so that the relative tire load $R_t(t) = k_t x_t(t)/(m_s + m_u)g$ can satisfy $|R_t(t)| \leq r_{tu} < 1$, where r_{tu} is a design parameter.

To develop a robust active suspension controller that can achieve the above conditions, the following assumptions are made for the vehicle (1).

A1 The elements of the state $\mathbf{x}(t)$ can be measured.

A2 The derivatives of the road displacement $z_r(t)^{(i)}$, $i = 0 \dots 2$ are unknown but bounded.

A3 Parameters m_u, k_s and c_s do not vary and are known.

A4 The nominal value \bar{k}_t is known, but k_t is unknown, and there exist known constants m_{sU} and m_{sL} such that $m_{sU} \geq m_s \geq m_{sL} > 0$. Sprung mass m_s can be measured, but there exist measurement errors.

3 Development of ideal vehicle model

To meet the design objective, we introduce an ideal vehicle model. Since the design scheme of the ideal vehicle model is very complex, we will explain the design scheme briefly. At first, we design two vehicle models $\mathbf{x}_i(t)$, $i = U, L$ given by

$$\left. \begin{aligned} \mathbf{x}_i(t) &= \mathbf{x}_{0i}(t) + \mathbf{d}\dot{\mathbf{x}}_b(t), \quad \mathbf{x}_{0i}(0) = \mathbf{x}(0) - \mathbf{d}\dot{\mathbf{x}}_b(0) \\ \dot{\mathbf{x}}_{0i}(t) &= \mathbf{A}_i\mathbf{x}_i(t) + \mathbf{b}\frac{1}{m_{si}}\mu_i(t) - \mathbf{d}\xi(t), \quad i = U, L \\ \mu_i(t) &= \mu_{ci}(t) + \mu_{ti}(t) \end{aligned} \right\} \quad (3)$$

$$\mathbf{A}_i = \begin{bmatrix} \Omega_b + \mathbf{b}_b\mathbf{a}_{1bi}^T & \mathbf{b}_b\mathbf{a}_{1ti}^T \\ -m_{siu}\mathbf{b}_t\mathbf{b}_b^T & \mathbf{A}_t \end{bmatrix}, \quad m_{siu} = \frac{m_{si}}{m_u}, \quad i = U, L, \quad (4)$$

where $\bar{\mathbf{A}}_t$ is a matrix in which k_{tu} in \mathbf{A}_t is replaced by $\bar{k}_{tu} = \bar{k}_t/m_u$, \mathbf{a}_{1bi} and \mathbf{a}_{1ti} are vectors in which the parameters k_{tu} and m_s of $c_s/m_s, k_s/m_s$ and m_s/m_u in \mathbf{a}_{1b} and \mathbf{a}_{1t} are replaced by \bar{k}_{tu} and m_{si} . The parameters \mathbf{a}_{1b} and \mathbf{a}_{1t} are defined in the fourth and fifth equations of (2). The parameters $m_{si}, i = U, L$ are defined in the assumption **A4**. Using $\dot{\mathbf{x}}_b(t) = \xi(t) - \ddot{z}_r(t)$ in (3), we have

$$\dot{\mathbf{x}}_i(t) = \mathbf{A}_i\mathbf{x}_i(t) + \mathbf{b}\frac{1}{m_{si}}\mu_i(t) - \mathbf{d}\ddot{z}_r(t), \quad \mathbf{x}_i(0) = \mathbf{x}(0). \quad (5)$$

In the vehicle model $x_U(t)$, the situation is considered where the sprung mass m_s becomes maximum m_U and in the vehicle model $x_L(t)$, the situation is considered where the sprung mass m_s becomes minimum m_L . The model inputs $\mu_i(t)$, $i = U, L$ are designed by using the same scheme proposed in [21]. After the two vehicle models are designed, to design an ideal vehicle model for varying sprung mass values, the two vehicle models are linearly combined.

The signal $\mu_{ci}(t)$, $i = U, L$ are input signals mainly to keep good ride comfort in each vehicle model, and are given by

$$\left. \begin{aligned} \mu_{ci}(t) &= -\frac{m_{si}}{r_{ci}} \mathbf{b}^T P_{ci} \mathbf{x}_i(t) \\ A_i^T P_{ci} + P_{ci} A_i - \frac{1}{r_{ci}} P_{ci} \mathbf{b} \mathbf{b}^T P_{ci} &= -Q_{ci} \end{aligned} \right\} \quad (6)$$

where $r_{ci} > 0$ and $Q_{ci} > 0$, $i = U, L$ are design parameters and set by using a trial and error method so that the sprung mass acceleration $|\xi_i(t)| = |[0 \ 0 \ 1 \ 0 \ 0] \mathbf{x}_i(t)|$ can become small in each vehicle model and the condition **C1** can be achieved.

Only in case of $|R_{ii}(t)| \geq r_u$ where $R_{ii}(t) = \bar{k}_i \mathbf{c}_i^T \mathbf{x}_{ii}(t) / (m_{si} + m_u) / g$ and r_u is a design parameter such that $1 > r_{iu} > r_u > 0$ (r_{iu} is design parameter defined in condition **C2.**), the input signals $\mu_{ii}(t)$, $i = U, L$ work so as to keep the relative tire loads in the range $|R_{ii}(t)| \leq r_{iu}$, and are given by

$$\left. \begin{aligned} \mu_{ii}(t) &= -m_{si} \beta_i f_\varepsilon(R_{ii}) \mathbf{b}^T P_{ii} \varepsilon_i(t) \\ &\quad + m_{si} f_\omega(R_{ii}) (\hat{\omega}_{\varepsilon 0i}(t) + \omega_{\varepsilon i}(t)) \\ A_{ci}^T P_{ii} + P_{ii} A_{ci} &= -Q_{ii}, \quad Q_{ii} > 0 \\ A_{ci} &= A_i - \frac{1}{r_{ci}} \mathbf{b} \mathbf{b}^T P_{ci} \end{aligned} \right\} \quad (7)$$

$$\left. \begin{aligned} \varepsilon_i(t) &= \mathbf{x}_i(t) - \mathbf{x}_{ri}(t), \quad \omega_{\varepsilon i}(t) = -\mathbf{b}^T A_{ci} \mathbf{x}_{ri}(t) \\ \mathbf{x}_{ri}(t) &= -\left[\frac{m_{si} + m_u}{m_{si}} \eta(t) \quad \frac{m_{si} + m_u}{m_{si}} \dot{\eta}(t) \quad \frac{m_u}{m_{si}} \hat{w}(t) \quad 0 \quad 0 \right]^T \\ \hat{\omega}_{\varepsilon 0i}(t) &= \mathcal{L}^{-1} \left[\frac{s}{T_r s + 1} \mathcal{L}[\mathbf{b}^T \mathbf{x}_{ri}(t)] \right] \end{aligned} \right\} \quad (8)$$

$$\left. \begin{aligned} \hat{w}(t) &= \ddot{\eta}(t), \\ \eta(t) &= \mathcal{L}^{-1} \left[\frac{1}{s^2 + 2\zeta_r \omega_r s + \omega_r^2} \frac{1}{T_r s + 1} \right. \\ &\quad \left. \times (\mathcal{L}[\xi(t)] - s\mathcal{L}[\dot{x}_b(t)]) \right] \end{aligned} \right\} \quad (9)$$

$$\left. \begin{aligned} f_\varepsilon(R_{ii}) &= \begin{cases} 0 & \text{if } |R_{ii}(t)| < r_u \\ |R_{ii}(t) - \text{sgn}(R_{ii})r_u| & \text{if } |R_{ii}(t)| \geq r_u \end{cases} \\ f_\omega(R_{ii}) &= \begin{cases} 0 & \text{if } |R_{ii}(t)| < r_u \\ 1 & \text{if } |R_{ii}(t)| \geq r_u \end{cases} \end{aligned} \right\} \quad (10)$$

where $T_r, \zeta_r, \omega_r, T_t > 0$, $\beta_i > 0$ and $Q_{ii} > 0$, $i = U, L$ are design parameters. In (9), $\hat{w}(t)$ denotes the estimate of $w(t) = \ddot{z}_r(t)$ [21]. The design parameters are determined by using a trial and error method so that the state norms $\|\varepsilon_i(t)\|$, $i = U, L$ defined in (8) can be reduced. If the state norms $\|\varepsilon_i(t)\|$ including the estimate $\hat{w}(t)$ of the load disturbance $w(t) = \ddot{z}_r(t)$ can be reduced, the tire deflections $|x_{ii}(t)| = |[0 \ 0 \ 0 \ 1 \ 0] \mathbf{x}_i(t)|$, $i = U, L$ can be reduced and the relative tire loads $|R_{ii}(t)|$ can be also reduced as shown in the reference paper [21].

To develop an ideal vehicle model $x_d(t)$ adaptable for any m_s , we will integrate the two vehicle models as

$$\left. \begin{aligned} \mathbf{x}_d(t) &= [\mathbf{x}_{bd}(t)^T \quad \mathbf{x}_{ld}(t)^T]^T = T_U \mathbf{x}_U(t) + T_L \mathbf{x}_L(t) \\ T_U &= \beta_m \text{diag} \left[\frac{m_{sU}}{\hat{m}_s} \quad \frac{m_{sU}}{\hat{m}_s} \quad \frac{m_{sU}}{\hat{m}_s} \quad 1 \quad 1 \right] \\ T_L &= (1 - \beta_m) \text{diag} \left[\frac{m_{sL}}{\hat{m}_s} \quad \frac{m_{sL}}{\hat{m}_s} \quad \frac{m_{sL}}{\hat{m}_s} \quad 1 \quad 1 \right] \end{aligned} \right\} \quad (11)$$

where \hat{m}_s is the measured value of m_s and β_m is a parameter determined by

$$\beta_m m_{sU} + (1 - \beta_m) m_{sL} = \hat{m}_s, \quad 1 \geq \beta_m \geq 0. \quad (12)$$

Lemma 1 The ideal vehicle model is given by

$$\left. \begin{aligned} \dot{\mathbf{x}}_d(t) &= \bar{A} \mathbf{x}_d(t) + \frac{1}{\hat{m}_s} \mathbf{b} \mu_d(t) - \mathbf{d} \ddot{z}_r(t), \quad \mathbf{x}_d(0) = \mathbf{x}(0) \\ \mu_d(t) &= \beta_m \mathbf{a}_{\mu U}^T \mathbf{x}_U(t) + (1 - \beta_m) \mathbf{a}_{\mu L}^T \mathbf{x}_L(t) \\ &\quad + \beta_m \mu_U(t) + (1 - \beta_m) \mu_L(t) \\ \mathbf{a}_{\mu i} &= [m_{si}(\mathbf{a}_{1bi} - \bar{\mathbf{a}}_{1b})^T \quad (m_{si} \mathbf{a}_{1ti} - \hat{m}_s \bar{\mathbf{a}}_{1t})^T]^T \end{aligned} \right\} \quad (13)$$

$$\bar{A} = \left[\begin{array}{cc} \bar{A}_b & \mathbf{b}_b \bar{\mathbf{a}}_{1t}^T \\ -\bar{m}_{su} \mathbf{b}_t \mathbf{b}_b^T & \bar{A}_t \end{array} \right], \quad \left. \begin{array}{l} \bar{A}_b = \Omega_b + \mathbf{b}_b \bar{\mathbf{a}}_{1b}^T \\ \bar{m}_{su} = \frac{\hat{m}_s}{m_u} \end{array} \right\} \quad (14)$$

where $\bar{\mathbf{a}}_{1b}$ and $\bar{\mathbf{a}}_{1t}$ are vectors in which the parameters k_{iu} and m_s of c_s/m_s , k_s/m_s and m_s/m_u in \mathbf{a}_{1b} and \mathbf{a}_{1t} are replaced by \bar{k}_{iu} and \hat{m}_s . The parameters \mathbf{a}_{1b} and \mathbf{a}_{1t} are depend in the fourth and fifth equations of (2).

Proof From (5), (11) and (12), we can derive (13) and (14) very easily. \square

It is expected that good ride comfort can be maintained in the ideal vehicle model for any sprung mass \hat{m}_s . This fact will be ascertained by using numerical simulation results. As for $R_{id}(t) = \bar{k}_t/(\hat{m}_s + m_u)/g \times \mathbf{c}_t^T \mathbf{x}_{id}(t)$, the relation $|R_{id}(t)| \leq r_{ru}$ holds for any sprung mass \hat{m}_s . Since model controllers (7)-(10) are designed so that the relations $|R_{ri}(t)| \leq r_{ru}$, $i = U, L$ can hold, for the relative tire load $R_{id}(t)$, we have

$$|R_{id}(t)| = \left| \frac{\beta_m(m_{sU} + m_u)}{\hat{m}_s + m_u} R_{iU}(t) + \frac{(1 - \beta_m)(m_{sL} + m_u)}{\hat{m}_s + m_u} R_{iL}(t) \right| \leq r_{ru}. \tag{15}$$

4 Development of controller

To force the real vehicle to track the ideal vehicle model, consider the tracking errors $\tilde{\mathbf{x}}_b(t) = \mathbf{x}_b(t) - \mathbf{x}_{bd}(t)$ and $\tilde{\mathbf{x}}_t(t) = \mathbf{x}_t(t) - \mathbf{x}_{td}(t)$. Then, we have

$$\begin{aligned} \dot{\tilde{\mathbf{x}}}_b(t) &= \bar{A}_b \tilde{\mathbf{x}}_b(t) + \frac{1}{m_s} \mathbf{b}_b (\mu(t) - \mu_d(t) + \hat{m}_s \bar{\mathbf{a}}_1^T \tilde{\mathbf{x}}_t(t)) \\ &\quad + \mathbf{b}_b (\tilde{\mathbf{e}}_b^T \tilde{\mathbf{x}}(t) + \tilde{e}_{bd}(t)), \quad \tilde{\mathbf{x}}_b(0) = [0 \ 0 \ 0]^T, \end{aligned} \tag{16}$$

$$\dot{\tilde{\mathbf{x}}}_t = A_t \tilde{\mathbf{x}}_t(t) - m_{su} \mathbf{b}_t \mathbf{b}_b^T \tilde{\mathbf{x}}_b(t) - \mathbf{b}_t \tilde{e}_{td}(t), \quad \tilde{\mathbf{x}}_t(0) = [0 \ 0]^T, \tag{17}$$

$$\left. \begin{aligned} \tilde{\mathbf{e}}_b &= \tilde{\mathbf{a}}_1 + \left[0 \ 0 \ 0 \ \frac{\tilde{m}_s}{m_s} \bar{\mathbf{a}}_{1t}^T \right]^T, \quad \mathbf{a}_1 = [\mathbf{a}_{1b}^T \ \mathbf{a}_{1t}^T]^T \\ \tilde{e}_{bd}(t) &= -\frac{\tilde{m}_s}{m_s \tilde{m}_s} \mu_d(t) + \tilde{\mathbf{a}}_1^T \mathbf{x}_d(t), \quad \tilde{\mathbf{a}}_1 = \mathbf{a}_1 - \bar{\mathbf{a}}_1 \\ \bar{\mathbf{a}}_1 &= [\bar{\mathbf{a}}_{1b}^T \ \bar{\mathbf{a}}_{1t}^T]^T, \quad \tilde{m}_s = m_s - \hat{m}_s, \quad \tilde{k}_{tu} = k_{tu} - \bar{k}_{tu} \\ \tilde{e}_{td} &= \tilde{k}_{tu} \mathbf{c}_t^T \mathbf{x}_{id}(t) + \frac{\tilde{m}_s}{m_u} \mathbf{b}_b^T \mathbf{x}_{bd}(t) \end{aligned} \right\}, \tag{18}$$

where $\tilde{\mathbf{e}}_b$ is bounded unknown vector, $\tilde{e}_{bd}(t)$ and $\tilde{e}_{td}(t)$ are bonded signals. The vector $\tilde{\mathbf{e}}_b$ and the signals $\tilde{e}_{bd}(t)$, $\tilde{e}_{td}(t)$ becomes zero if $\tilde{k}_{tu} = 0$ and $\tilde{m}_s = 0$.

To develop a robust active suspension controller, consider the state given by

$$\left. \begin{aligned} \boldsymbol{\varepsilon}_b(t) &= \tilde{\mathbf{x}}_b(t) - \mathbf{x}_c(t), \quad \boldsymbol{\varepsilon}_b(0) = [0 \ 0 \ 0]^T \\ \mathbf{x}_c(t) &= \frac{\beta_{ic}}{m_{su}} \left[\int_0^t \mathbf{c}_t^T \tilde{\mathbf{x}}_t(\tau) d\tau \right. \\ &\quad \left. \mathbf{c}_t^T \tilde{\mathbf{x}}_t(t) \ \mathbf{b}_t^T \tilde{\mathbf{x}}_t(t) \right]^T, \end{aligned} \right\} \tag{19}$$

where $\beta_{ic} \geq 1$ is a design parameter. Then, we have

$$\begin{aligned} \dot{\boldsymbol{\varepsilon}}_b(t) &= \bar{A}_b \boldsymbol{\varepsilon}_b(t) + \frac{1}{m_s} \mathbf{b}_b (\mu(t) - \mu_d(t) \\ &\quad + \hat{m}_s \bar{\mathbf{a}}_{1b}^T \mathbf{x}_c(t) + \bar{\mathbf{a}}_{1t}^T \tilde{\mathbf{x}}(t)) \\ &\quad + \mathbf{b}_b \left(\tilde{e}_{ed}(t) + \tilde{\mathbf{e}}_e^T \tilde{\mathbf{x}}(t) + \frac{\tilde{m}_s}{m_s} \bar{\mathbf{a}}_{1b}^T \mathbf{x}_c(t) \right), \end{aligned} \tag{20}$$

$$\dot{\tilde{\mathbf{x}}}_t(t) = A_{ic} \tilde{\mathbf{x}}_t(t) - m_{su} \mathbf{b}_t \mathbf{b}_b^T \boldsymbol{\varepsilon}_b(t) - \mathbf{b}_t \tilde{e}_{td}(t), \tag{21}$$

$$\left. \begin{aligned} \bar{\mathbf{a}}_e &= \hat{m}_s [0 \ 0 \ 0 \ \bar{\mathbf{a}}_{1t}^T]^T + \beta_{ic} [\hat{m}_s \mathbf{b}_b^T \ m_u \bar{k}_{tu} \mathbf{c}_t^T]^T \\ \tilde{e}_{ed}(t) &= \tilde{e}_{bd}(t) + \frac{\beta_{ic}}{m_{su}} \tilde{e}_{td}(t), \quad A_{ic} = A_t - \frac{\beta_{ic} m_s}{\hat{m}_s} \mathbf{b}_t \mathbf{b}_t^T \\ \tilde{\mathbf{e}}_e &= \tilde{\mathbf{e}}_b \\ &\quad + \beta_{ic} \left[\frac{\tilde{m}_s (m_s + \hat{m}_s)}{m_s \hat{m}_s} \mathbf{b}_b^T \ \frac{1}{m_{su}} \left(\tilde{k}_{tu} + \frac{\tilde{m}_s \bar{k}_{tu}}{m_s} \right) \mathbf{c}_t^T \right]^T \end{aligned} \right\}. \tag{22}$$

Although the system matrix A_t is not a stable matrix, the system matrix A_{ic} becomes an asymptotically stable matrix due to introduction of the signal $\boldsymbol{\varepsilon}_b(t)$ including the signal $\mathbf{x}_c(t)$. If the signal $\boldsymbol{\varepsilon}_b(t)$ becomes stable and small, then the state $\tilde{\mathbf{x}}_t(t)$ becomes also stable because the signal $\tilde{e}_{td}(t)$ is bounded.

Based on the tracking error systems (20) and (21), a robust controller is developed as

$$\left. \begin{aligned} \dot{u}(t) &= -\alpha u(t) + \mu(t) \\ \mu(t) &= \mu_d(t) - \hat{m}_s \bar{\mathbf{a}}_{1b}^T \mathbf{x}_c(t) - \bar{\mathbf{a}}_{1t}^T \tilde{\mathbf{x}}(t) \\ &\quad - \hat{m}_s \beta_c (\beta_c + \|\tilde{\mathbf{x}}(t)\|^2 + \|\mathbf{x}_c(t)\|^2) \mathbf{b}_b^T P \boldsymbol{\varepsilon}_b(t) \\ \bar{A}_b^T P + P \bar{A}_b &= -Q, \quad \beta_c \geq 1, \quad Q > 0 \end{aligned} \right\}, \tag{23}$$

where β_c and Q are design parameters. For $\alpha > 0$, since the matrix \bar{A}_b becomes a Hurwitz matrix, Lyapunov equation has a positive definite matrix $P > 0$.

For the controlled vehicle system (20), (21) and (23), we have the following theorem.

Theorem 1 *In case of $\tilde{m}_s = 0$ and $\tilde{k}_t = k_t - \bar{k}_t = 0$, we obtain $\|\tilde{\mathbf{x}}(t)\| = 0$, where \tilde{m}_s is defined in the third equation of (18).*

In case of $\tilde{m}_s \neq 0$ or $\tilde{k}_t \neq 0$, the tracking error $\tilde{\mathbf{x}}(t)$ becomes stable. In addition to the fact, there exists a constant value $\rho_\varepsilon \geq 0$ independent of the design parameter β_c such that $\|\boldsymbol{\varepsilon}_b(t)\|^2 \leq \rho_\varepsilon / \beta_c$.

Proof At first, we will show $\|\tilde{\mathbf{x}}(t)\| = 0$ in case of $\tilde{m}_s = 0$ and $\tilde{k}_t = 0$. Since $\|\tilde{\mathbf{e}}_e\| = 0$ and $\tilde{e}_{ed}(t) = 0$, the derivative of the positive definite function $V(t) = \boldsymbol{\varepsilon}_b(t)^T P \boldsymbol{\varepsilon}_b(t)$ is given by

$$\begin{aligned} \dot{V}(t) = & -\varepsilon_b(t)^T Q \varepsilon_b(t) - 2 \frac{\hat{m}_s}{m_s} \beta_c (\beta_c + \|\tilde{\mathbf{x}}(t)\|^2) \\ & + \|\tilde{\mathbf{x}}_c(t)\|^2 \varepsilon_b(t)^T P \mathbf{b}_b \mathbf{b}_b^T P \varepsilon_b(t). \end{aligned} \tag{24}$$

From (24) and $\|\varepsilon_b(0)\| = 0$, we can obtain $\|\varepsilon_b(t)\| = 0$. In (21), the matrix A_{ic} includes uncertainties but asymptotically stable. In addition to the fact, since $\tilde{e}_{id}(t) = 0$ and $\|\tilde{\mathbf{x}}_i(0)\| = 0$, we can conclude that $\|\tilde{\mathbf{x}}(t)\| = 0$.

Next, in case of $\tilde{m}_s \neq 0$ or $\tilde{k}_t \neq 0$, we will show that $\tilde{\mathbf{x}}(t)$ becomes stable. The derivative of $V(t)$ is given by

$$\begin{aligned} \dot{V}(t) = & -\varepsilon_b(t)^T Q \varepsilon_b(t) - 2 \frac{\hat{m}_s}{m_s} \beta_c (\beta_c + \|\tilde{\mathbf{x}}(t)\|^2 + \|\tilde{\mathbf{x}}_c(t)\|^2) \\ & \times \varepsilon_b(t)^T P \mathbf{b}_b \mathbf{b}_b^T P \varepsilon_b(t) + 2 \varepsilon_b(t)^T P \mathbf{b}_b \\ & \times \left(\tilde{e}_{ed}(t) + \tilde{\mathbf{e}}_\varepsilon^T \tilde{\mathbf{x}}(t) + \frac{\tilde{m}_s}{m_s} \tilde{\mathbf{a}}_{1b}^T \mathbf{x}_c(t) \right). \end{aligned} \tag{25}$$

Since $\tilde{e}_{ed}(t), \|\tilde{\mathbf{e}}_\varepsilon\|, \tilde{m}_s/m_s, \|\tilde{\mathbf{a}}_{1b}\|$ are bounded and $\beta_c \geq 1$, there exists a constant $\rho_{\varepsilon 1}$ independent of design parameter β_c such that the second and third terms of the right side of (25) are less than and equal to $\rho_{\varepsilon 1}/\beta_c$. Using the fact in (25), we can obtain

$$\dot{V}(t) \leq -\delta_\varepsilon V(t) + \frac{\rho_{\varepsilon 1}}{\beta_c}, \quad \delta_\varepsilon = \frac{\lambda_{\min}[Q]}{\lambda_{\max}[P]}. \tag{26}$$

From (26), $\varepsilon_b(t)$ is stable and we can have $\|\varepsilon_b(t)\|^2 \leq \rho_\varepsilon/\beta_c$, $\rho_\varepsilon = \rho_{\varepsilon 1}/(\delta_\varepsilon \lambda_{\min}[P])$. From (21), we can obtain that the tracking error $\tilde{\mathbf{x}}_i(t)$ is also stable, and then, we have from (19) that $\mathbf{b}_b^T \tilde{\mathbf{x}}_b(t)$ and $\mathbf{d}_b^T \tilde{\mathbf{x}}_b(t)$ are stable.

Multiplying $[0 \ 0 \ 0 \ \mathbf{b}_i^T]$ in the first equation of (13) from left and integrating, we have

$$\mathbf{b}_i^T \tilde{\mathbf{x}}_{id}(t) = -\bar{k}_{iu} \int_0^t \mathbf{c}_i^T \tilde{\mathbf{x}}_{id}(\tau) d\tau - \bar{m}_{su} \mathbf{d}_b^T \mathbf{x}_{bd}(t) - \dot{z}_r(t). \tag{27}$$

From assumption A2 and (27), $\int_0^t \mathbf{c}_i^T \tilde{\mathbf{x}}_{id}(\tau) d\tau$ is bounded, and then, we can have that $\int_0^t \tilde{e}_{id}(\tau) d\tau$ is also bounded. Using the facts in the relation obtained by multiplying \mathbf{b}_i^T in (17) from left and integrating, we have that $\int_0^t \mathbf{c}_i^T \tilde{\mathbf{x}}_i(\tau) d\tau$ is bounded, and then, we can conclude that $\tilde{\mathbf{x}}(t)$ is stable. \square

From theorem 1, in case of $\tilde{m}_s = 0$ and $\tilde{k}_t = 0$, good performance can be assured without redesign of the controller even if vehicle mass varies greatly. In case of $\tilde{m}_s \neq 0$ or $\tilde{k}_t \neq 0$, if $|\tilde{e}_{id}(t)|$ is small, it can be expected that as the design parameter β_c becomes large, $\|\tilde{\mathbf{x}}_i(t)\|$ and $|\mathbf{b}_b^T \tilde{\mathbf{x}}_b(t)|$ become small. The control performance in case of $\tilde{m}_s \neq 0$ or $\tilde{k}_t \neq 0$ are shown in the next section. When measurements errors exist in practical applications, there is a

possibility where large vibrations occur for a high feedback gain β_c .

5 Numerical simulation results

The numerical simulations are carried out to confirm usefulness of the proposed robust active suspension controller. The nominal vehicle parameter values are shown in Table 2 [21].

The design parameters of (9) and a controller (23) are set as $T_r = 0.01, \omega_r = 2, \zeta_r = 1$ and $\alpha = 1, Q = I$. The road surface displacement $z_r(t)$ is given by

$$\dot{z}_r(t) = -\frac{1}{T_{zr}} z_r(t) + \frac{1}{T_{zr}} w_r(t), \quad T_{zr} = 0.005 \tag{28}$$

$$w_r(t) = \begin{cases} \frac{h_z}{2} \left(\sin \left(\omega_z t - \frac{\pi}{2} \right) + 1 \right) & \text{if } 0 \leq t \leq \frac{2\pi}{\omega_{zr}} \\ 0 & \text{if } \frac{2\pi}{\omega_{zr}} < t \end{cases}, \tag{29}$$

where h_z is the amplitude and ω_z is the frequency of the uneven road surface.

The design parameters for an ideal vehicle model are set so that the conditions C1 and C2 can be achieved in the range of $h_z \in [9 \ 13]$ [cm] and $\omega_z \in [0.5 \ 3.5]$ [Hz].

$$\left. \begin{aligned} Q_U &= Q_b Q_b^T + 10^3 \mathbf{q}_a \mathbf{q}_a^T + Q_s \text{diag}[10^5 \ 10] Q_s^T \\ &\quad + 10^5 Q_u \text{diag}[1 \ 0.3] Q_u \\ Q_{iU} &= Q_b Q_b^T + \mathbf{q}_a \mathbf{q}_a^T + Q_s Q_s^T + Q_u Q_u^T \\ \mathbf{q}_a &= [0 \ 0 \ 1 \ 0 \ 0]^T, \quad Q_s = Q_b - Q_t \\ Q_b &= \begin{bmatrix} 1 & 0 & 0 & 0 & 0 \\ 0 & 1 & 0 & 0 & 0 \end{bmatrix}^T, \quad Q_u = \begin{bmatrix} 0 & 0 & 0 & 1 & 0 \\ 0 & 0 & 0 & 0 & 1 \end{bmatrix}^T \\ \beta_U &= m_s 10^7, \quad m_{sU} = \bar{m}_s + 65 \end{aligned} \right\}, \tag{30}$$

$$\left. \begin{aligned} Q_L &= Q_b Q_b^T + 10^3 \mathbf{q}_a \mathbf{q}_a^T + Q_s \text{diag}[10^5 \ 10] Q_s^T \\ &\quad + 6 \times 10^6 Q_u \text{diag}[1 \ 0.3] Q_u \\ Q_{iL} &= Q_{iU}, \quad \beta_L = m_s 10^7, \quad m_{sL} = \bar{m}_s - 65 \end{aligned} \right\}. \tag{31}$$

In the designed models, the parameters r_{iu} and r_u are set as $r_{iu} = 0.6$ and $r_u = 0.45$.

In the matrixes $Q_i, i = U, L$, to meet C1 in each vehicle model (5), coefficients of $\mathbf{q}_a \mathbf{q}_a^T$ are set to be a large value. However, when the coefficients of $\mathbf{q}_a \mathbf{q}_a^T$ are only set to be large, vibrations appear in suspension stroke and tire deflection. To avoid the vibrations, coefficients corresponding to Q_s and Q_u are also set to be large values. To meet C2, we mainly use high feedback gains $\beta_i, i = U, L$

in each vehicle model (5). The coefficients in $Q_{ii}, i = U, L$ are set to be one.

We can set any values of m_{sU} and m_{sL} . When a nominal situation has two passengers in standard-size vehicles, it is considered that increase/decrease of the sprung mass may about 15 [%]. Under the notion, we set the values of m_{sU} and m_{sL} .

Figure 2 a–f shows variations of maximum values of $|R_t(t)|$ and $|\xi(t)|$ of the passive vehicle ($u(t) = 0$). Figure 2g–l shows variations of maximum values of $|R_{td}(t)|$ and $|\xi_d(t)| = |\mathbf{b}^T \mathbf{x}_d(t)|$ of the ideal vehicle model. In the passive vehicle, the values of vehicle parameters are nominal values except the sprung mass m_s . In Fig. 2, x-axis denotes amplitude h_z [cm] and y-axis denotes frequency ω_z [Hz] of road surface displacement $z_r(t)$. In Fig. 2a,c,e, for clarity, the maximum relative tire loads are set as $\max |R_t(t)| = 0.8$ in the case when $\max |R_t(t)| > r_{tu} = 0.6$.

As shown in Fig. 2 a,c,e in the passive vehicle, handling performance becomes very poor ($|R_t(t)| > r_{tu} = 0.6$) in some regions of h_z and ω_z . Compared with the passive vehicle, the performance of the designed ideal vehicle model becomes

much better. In addition to the fact, by setting the measured vehicle mass \hat{m}_s , we can easily obtain the ideal vehicle model with high performance compared with passive vehicle without redesigning.

In the case of $m_s = \hat{m}_s$ and $k_t = \bar{k}_t$, as shown in Theorem 1, the behavior of the controlled vehicle and an ideal vehicle model becomes the same. Therefore, consider the case where there exist uncertainties such as $m_s = \hat{m}_s(1 + \Delta_m/100)$ and $k_t = \bar{k}_t(1 + \Delta_k/100)$, where Δ_m and Δ_k denote measured error and parameter uncertainty. In case of $\hat{m}_s = 320$ [kg], $\omega_z = 2$ [Hz], $h_z = 13$ [cm] $\Delta_m = 5$ [%] and $\Delta_k = -10$ [%], Fig. 3 shows responses of the controlled vehicle for various β_c . In Fig. 3 a,b, thick solid lines show responses of the ideal vehicle model. When Δ_k becomes larger than 10 [%], the maximum value of $|R_t(t)|$ becomes larger and the maximum value of $|\xi(t)|$ becomes smaller. If Δ_k becomes too large, the maximum value of $|R_t(t)|$ exceeds r_{tu} . When Δ_m becomes smaller than -10 [%], the maximum value of $|R_t(t)|$ becomes larger and the maximum value of $|\xi(t)|$ becomes larger. If Δ_m

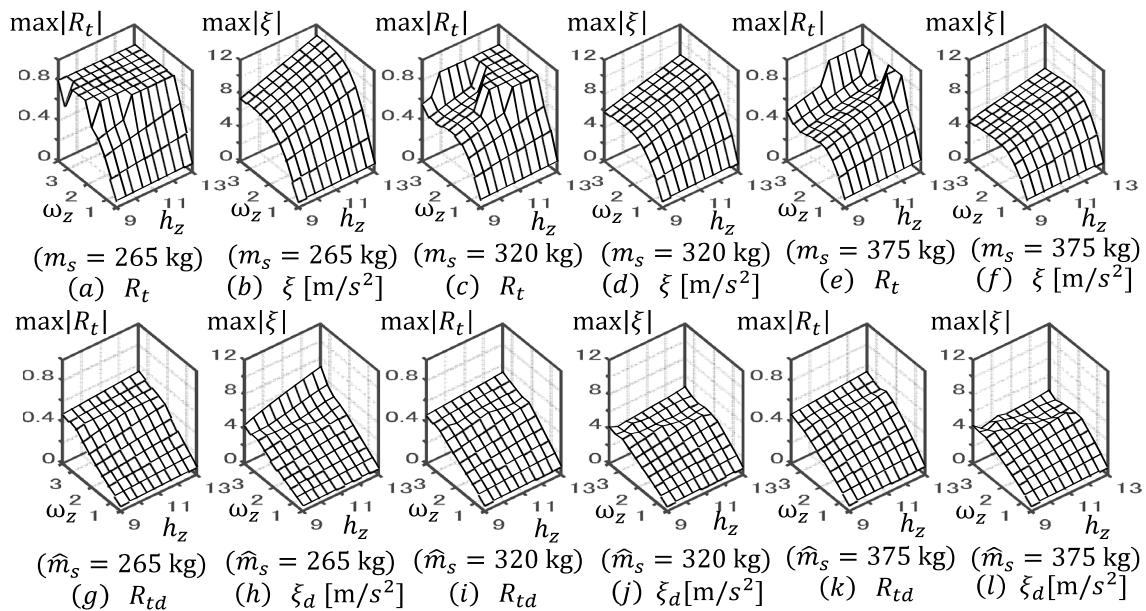
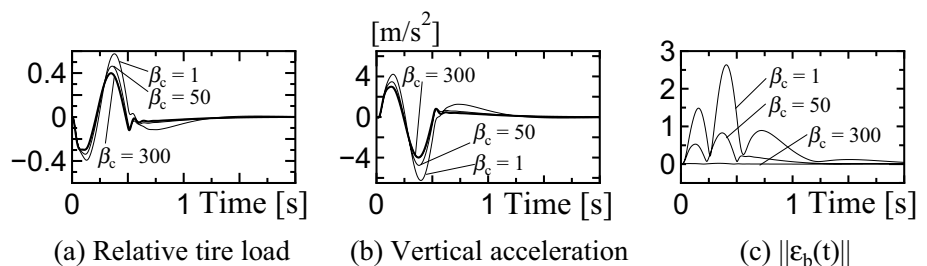


Fig. 2 Passive vehicle and ideal vehicle model

Fig. 3 Responses of controlled vehicle



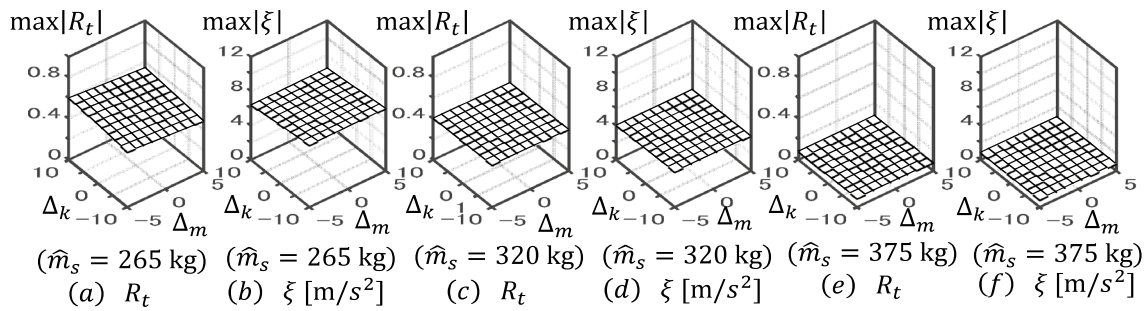


Fig. 4 Robust performance of controlled vehicle

becomes too small, the maximum value of $|\xi(t)|$ becomes very large.

As shown in Fig. 3 c, the maximum error of $\|\varepsilon_b(t)\|$ becomes small as the design parameter β_c becomes larger.

Table 2 Nominal values of vehicle parameters

\bar{m}_s, \bar{m}_u	320	kg	40	kg
\bar{k}_s, \bar{c}_s	18000	N/m	1000	Ns/m
\bar{k}_t	200000	N/m		

When β_c is 300, the maximum error of $\|\varepsilon_b(t)\|$ becomes almost zero. As shown in Fig. 3 a,b, as the β_c becomes larger, the error between the controlled vehicle and the ideal vehicle model becomes smaller.

To investigate the effects of uncertainties Δ_m and Δ_k on the controlled vehicle, in Fig. 4, we show variations of maximum values of $|R_t(t)|$ and $|\xi(t)|$ for various Δ_m and Δ_k . In the controlled vehicle, the design parameter is set as $\beta_c = 300$. In Fig. 4, x-axis denotes Δ_m and y-axis denotes Δ_k .

As shown in Fig. 4, even if there exist measured errors in \hat{m}_s , steering performance and ride comfort little vary, while, as shown in Fig. 4 a, as Δ_k becomes large, the maximum values of $|R_t(t)|$ becomes large and close to $r_{tu} = 0.6$. However, as Δ_k becomes small, the maximum values of $|R_t(t)|$ become small. The variations of $|\xi(t)|$ against the variations of Δ_k become small as shown in Fig. 4 b,d,f.

From the facts stated above, we can conclude that in the case when $|\Delta_m| \leq 5\%$ and $|\Delta_k| \leq 10\%$, in the controlled vehicle, good handling performance and good ride comfort can be maintained even if vehicle masses vary greatly.

6 Conclusion

We proposed a design method of an ideal vehicle model in which good steering performance and good ride comfort can be maintained even if vehicle mass varies greatly. To

achieve a good control performance, a robust tracking controller is developed to force the actual vehicle follow the ideal vehicle model. Using numerical simulation results, it is shown that in the case for small uncertainties, good handling performance and good ride comfort can be maintained in the controlled vehicle even if vehicle mass varies greatly.

References

1. Wang Q, Oya M, Jin Z, Kobayashi T (2005) Adaptive lane keeping control of vehicles, Proceedings of SICE annual conference 2005, Okayama, Japan, pp 2200–2204, 2005
2. Wang Q, Oya M, Kobayashi T (2008), Adaptive lane keeping control for combination vehicles without measurement of lateral velocity. In: Proceedings of advances in vehicle control and safety, Kobe, Japan, pp 331–336
3. Toro O, Becsi T, Aradi S (2016) Design of lane keeping algorithm of autonomous vehicle. Period Polytech Transp Eng 44(1):60–68
4. Sun W, Gao H, Kaynak O (2011) Finite frequency H_∞ control for vehicle active suspension systems. IEEE Trans Control Syst Technol 19(2):416–422
5. Koch G, Kloiber T (2014) Driving state adaptive control of an active vehicle suspension system. IEEE Trans Control Syst Technol 22(1):44–57
6. Brezas P, Smith MC (2014) Linear quadratic optimal and risk-sensitive control for vehicle active suspensions. IEEE Trans Control Syst Technol 22(2):543–556
7. Metered H, Sika Z (2015) Vibration control of vehicle active suspension using sliding mode under parameters uncertainty. J Traffic Logist Eng 3(2):136–142
8. Vajayanti S, Deshpande P, Shendge D, Phadke SB (2016) Dual objective active suspension system based on a novel nonlinear disturbance compensator. Veh Syst Dyn 54(9):1269–1290
9. Rath JJ, Defoort M, Karimi HR, Veluvolu KC (2017) Output feedback active suspension control with higher order terminal sliding mode. IEEE Trans Industr Electron 64(2):1392–1403
10. Wu J-L (2017) A simultaneous mixed LQR/ H_∞ control approach to the design of reliable active suspension controllers. Asian J Control 19(2):415–427
11. Xue W, Li K, Chen Q, Liu L (2019) Mixed FTS/ H_∞ control of vehicle active suspensions with shock road disturbance. Veh Syst Dyn 57(6):841–854
12. Lin B, Su X, Li X (2019) Fuzzy sliding mode control for active suspension system with proportional differential sliding mode observer. Asian J Control 21(1):264–276
13. Cao Z, Zhao W, Hou X, Chen Z (2020) Multi-objective robust control for vehicle Active suspension systems via parameterized controller. IEEE Access 8:7455–7465

14. Meng Q, Chen C-C, Wang P, Sun Z-Y, Li B (2021) Study on vehicle active suspension system control method based on homogeneous domination approach. *Asian J Control* 23:561–571
 15. Oya M, Harada H, Araki Y (2007) An active suspension controller achieving the best ride comfort at any specified location on a vehicle. *J Syst Design Dyn* 2:245–256
 16. Oya M, Tsuchida Y, Wang Q, Taira Y (2008) Adaptive active suspension controller achieving the best ride comfort at any specified location on vehicles with parameter uncertainties. *Int J Adv Mechatron Syst* 1(2):125–136
 17. Liu S, Zheng T, Zhao D, Hao R, Yang M (2020) Strongly perturbed sliding mode adaptive control of vehicle active suspension system considering actuator nonlinearity, Published Online, 03 Nov, *Veh Syst Dyn*
 18. Oya M, Okura R, Shibata H, Okumura K (2011) Robust control of vehicle active suspension systems. *ICIC Express Lett* 6:1019–1026
 19. Hu Y, Chen MZQ, Hou Z (2015) Multiplexed model predictive control for active vehicle suspensions. *Int J Control* 88(2):347–363
 20. Attia T, Vamvoudakis KG, Kochersberger K, Bird J, Furukawa T (2019) Simultaneous dynamic system estimation and optimal control of vehicle active suspension. *Veh Syst Dyn* 57(10):1467–1493
 21. Wang Y, Oya M, Taira Y (2022) A new active suspension control scheme for vehicles considering steering stability. *Int J Artif Life Robot* 27–4:812–817
 22. Metered H, Sika Z (2015) Vibration control of vehicle active suspension using sliding mode under parameters uncertainty. *J Traffic Logist Eng* 3(2):136–142
 23. Ovalle L, Rios H, Ahmed H (2022) Robust control for an active suspension system via continuous sliding-mode controllers. *Eng Sci Technol Int J* 28:101026
 24. Ahmad I, Ge X, Han Q-L (2022) Communication-constrained active suspension control for networked in-wheel motor-driven electric vehicles with dynamic dampers. *IEEE Trans Intell Veh* 7(3):590–602
- Publisher's Note** Springer Nature remains neutral with regard to jurisdictional claims in published maps and institutional affiliations.
- Springer Nature or its licensor (e.g. a society or other partner) holds exclusive rights to this article under a publishing agreement with the author(s) or other rightsholder(s); author self-archiving of the accepted manuscript version of this article is solely governed by the terms of such publishing agreement and applicable law.